Impact of Electrode Rotation on Aluminum GMAW Bead Shape

The rotating electrode pulsed GMAW process was investigated to improve argon shielding fusion characteristics and reduce helium usage

BY J. HANSEN AND D. D. HARWIG

Abstract

Aluminum gas metal arc welding (GMAW) uses inert shielding gas to minimize weld pool oxidation and reduce susceptibility to porosity and incomplete fusion defects. For aluminum shipbuilding, naval welding requirements highly recommend the use of helium-argon mixtures or pure helium shielding gas to provide a broader heat field and better weld toe fusion. Pure argon shielding gas can be used but has been susceptible to incomplete fusion and porosity defects, where argon's lower thermal conductivity promotes a narrower arc heat field and shallow weld fusion depth. Using helium is a concern because it is a finite resource that costs approximately five times more than argon.

The rotating electrode pulsed GMAW process was investigated to improve argon shielding fusion characteristics and reduce helium usage. Argon-shielded bead-on-plate tests were used to evaluate the relationship between ER5183 electrode rotation parameters and arc power on constant deposit area bead shape. These tests were compared to stringer beads (no oscillation) that were made with argon, helium, and helium-argon shielding gases. Electrode rotation improved underbead fusion depth width and toe fusion. With preferred rotation parameters, the bead width and incomplete fusion at weld toes were equivalent to helium-based welds. For weld reinforcement, electrode rotation promoted a nonsymmetric profile with deposit bias on the bead side, where rotation direction was aligned with travel direction. The bead-side deposit bias is an advantage based on preliminary horizontal V-groove welding procedures using ceramic backing. Electrode rotation can offset the effects of gravity, promoting a smoother bead and fusion profile.

Keywords

- Gas Metal Arc Welding
- Rotating Electrode Pulsed Gas Metal Arc Welding
- Aluminum Welding
- Shipyard Welding

Introduction

Aluminum structure fabrication brings new challenges to production, especially in shipbuilding, where large erection weld joints must be joined in all positions. Gas metal arc welding (GMAW) of aluminum poses significant issues without proper procedures in place. Current naval requirements (Ref. 1) for aluminum welding strongly recommend the use of pure helium or helium-argon mixtures to broaden the heat field and improve fusion characteristics. Pure argon shielding gas can be used, but welding experience has found that procedures using this gas are more susceptible to incomplete fusion and porosity. Argon-shielded arcs have a narrower heat field compared to helium-shielded arcs, so fusion quality can be an issue with the latter and especially on materials that have high thermal conductivity, like aluminum (Ref. 2). These issues are intensified when welding at high currents on thick plate sections. In particular, weld toe fusion quality is an issue as is bead overlap fusion when filling a groove. Argon GMAW is needed to reduce costs as helium is a finite resource that costs approximately five times more than argon.

Weld soundness, which implies complete fusion and defect-free weldments, is essential in erection welding of

large aluminum structures. One way to improve weld fusion bead shape is to oscillate or manipulate the arc to change the heat distribution, which then affects pool fusion depth, base metal dilution (BMD), and underbead shape. Previous research has analyzed the ability of magnetic arc oscillation to improve toe fusion characteristics (Ref. 3). Arc oscillation distributes heat over a larger weld pool area, improving fusion quality at the weld toes. Rotating electrode pulsed GMAW (REP-GMAW) has the potential to mitigate the need for helium shielding gas to ensure fusion quality. Here, the contact tip is rotated inside the welding gun nozzle to distribute the heat. The REP-GMAW gun offers the ability to vary rotation diameter and speed independently. Since the moving part is just the contact tip assembly, the rotation frequency can be very high compared to conventional transverse gun oscillation or weaving used in mechanized welding systems.

This investigation developed relationships between rotating electrode parameters and bead shape for argon-shielded bead-on-plate (BOP) deposits made with aluminum electrode ER5183. Preferred REP-GMAW parameters were compared to pulsed GMAW (GMAW-P) stringer bead BOP tests that were performed using pure argon, helium-argon, and helium shielding gases. Preliminary groove weld tests were also performed to support the transition of this technology for erection welding in flat and horizontal positions.

Background

GMAW Shielding Gas

The shielding gas chosen to generate an arc and protect the weld pool during welding heavily affects the mode of metal transfer and heat input (Refs. 4–6). The shielding gas also affects weld bead shape, metallurgical and mechanical properties, and the level of fume emissions (Refs. 7, 8). Two of the most common shielding gases used for GMAW of aluminum are argon and helium because they are inert and protect the molten pool. Argon gas is substantially heavier and more efficient in shielding the pool than helium. It is necessary to use two to three times the flow rate for helium to match the shielding provided by argon. Helium does provide the distinct advantage of higher thermal conductivity, which increases the heat field and improves weld bead shape. At arc temperatures, helium's thermal conductivity is two to four times that of argon's (Ref. 9). For shielding gases such as helium and argon, mass diffusivity of the atoms controls the thermal conductivity of the arc. The thermal diffusivity is equal to the inverse of the square root of the mass of the atom (Refs. 10, 11). Because argon has an atomic weight that is ten times that of helium's, the thermal conductivity of argon is 30% of helium's. This means that helium will conduct three times the heat across the arc when compared to argon. In 1989, Giedt et al. studied the melting efficiency of argon arc welding processes and found that base metal melting efficiency was incredibly low, normally around 20% or less (Ref. 12). Helium shielding gas increases heat supplied across the arc by 40% and can double the volume of melted metal (Ref. 13). Helium and argon-helium shielding gas mixtures are used to improve the arc heat field, BMD, and underbead

shape (Ref. 6). Argon-shielded arcs promote a narrower weld deposit that will exhibit finger-fusion depth with increasing current (Ref. 7).

REP-GMAW

REP-GMAW offers several advantages compared to stringer bead deposition with conventional welding guns. REP-GMAW is set up like a normal GMAW gun with the exception that electrode rotation controls are added to rotate the contact tip and electrode over a weld pool area. The first-generation REP-GMAW gun used a fixed rotating (spin) diameter with variable frequency via servo-motors (Ref. 14). A key benefit of the first-generation gun was improved weld joint tracking ability, especially on small fillet welds at high speeds. Here, high-speed rotation improved arc length sidewall sensing via higher signal-to-noise voltage signals. The higher signal strength was a result of power source reactance where the voltage change at the sidewalls increased with increasing rotation speed due to power source dynamics. High-speed arc rotation also improved weld bead shape as well as the fusion depth profile of the weld underbead (Ref. 14). Arc rotation also enhanced the ability to weld out of position, both horizontally and vertically, increasing production efficiency (Ref. 15). It has also been found that when rotating an arc, it is possible to increase weldment hardness through better and more uniform grain size refinement (Ref. 14).

The REP-GMAW process adds three variables to the P-GMAW procedure. These are spin diameter, spin frequency, and spin direction. The spin diameter is the circular profile the welding electrode travels while it is being rotated around the gun's centerline. The spin frequency is the number of spins per unit time measured in Hz or RPM. The spin direction determines whether the wire is traveling in a clockwise or counterclockwise rotation relative to the welding direction. Because arc rotation allows for increased fusion with groove sidewalls, it is possible to use a reduced bevel angle, allowing for cost savings on machining (Ref. 16). While the rotation of the arc assists with sidewall fusion depth within the joint, this does not come without a decrease in fusion depth in the root of the weld (Ref. 17). The REP-GMAW parameters must be optimized to ensure adequate fusion depth and fusion across the weld fusion depth profile (Refs. 18, 19). Surface contamination and porosity are also concerns when welding aluminum. Arc rotation assists in alleviating some of these issues by disrupting contamination on the surface of the weld pool (Ref. 20).

Experimental Procedures

This investigation evaluated the effects of rotating electrode (spin) variables on the resulting bead shape and fusion quality of GMAW-P ER5183 deposits. First, a shielding gas study was conducted using BOP tests to compare constant deposit area stringer beads using four different shielding gases: argon, 75% argon-25% helium, 50% Ar-50% He, and helium at three wire feed speed (WFS) levels. These shielding gas BOP tests were performed without electrode rotation. Then, REP-GMAW BOP study was used to compare two different spin diameters using pure argon at the same three WFS and travel speed (TS) levels.

Fig. 1 — REP-GMAW equipment setup. Bug-O tractor with OTC Welbee 500 GMAW power source and wire feeder.

All BOP welds were completed in the 1G position using an ER5183 electrode that was 1.6 mm (0.06 in.) in diameter. The deposit area was held constant by using a constant WFS to TS ratio of 20. The average arc power and heat input was approximately constant at each WFS by using the same constant current pulse waveform and arc length trim settings. The arc length varied depending on the shielding gas at each WFS, but the approach evaluated the effects of power and shielding gas on weld bead fusion quality.

Preferred spin parameters were then selected to evaluate feasibility and discuss the potential for welding horizontal V-groove butt joints on 16-mm (0.62-in.) ER5083. Visual and metallographic sections were used throughout the investigation to characterize bead shape quality. The bead's height, width, fusion depth, BMD, and toe incomplete fusion were measured for each test. Observations were also made to evaluate underbead fusion depth and bead reinforcement profiles. Bead shape maps and graphical relationships were developed by visually examining completed tests and characterizing weld cross-sectional bead shapes and fusion quality.

In addition, 32-mm-thick (1.25-in.-thick) plates of 5083 Aluminum were used for BOP tests and provided a significant heat sink. The surfaces of the plates were cleaned using an abrasive wheel to remove scale. Abrasive surface cleaning was performed immediately before each BOP test to ensure that the welds were always fabricated on constant base metal surface conditions. After abrasive grinding, the plates were degreased with acetone wipes. The plates were allowed to cool to room temperature between tests so there were no interpass temperature effects.

Equipment Setup

Figure 1 shows a photograph of the setup used for the bead shape study. The plate was fixed to the table using a C-clamp, ensuring that it did not move during testing. An OTC WB-P500L pulse power source was used, operating on the hard aluminum setting, with a trim setting of zero. The power source was operated in synergic mode, where the WFS was set on the power

Fig. 2 — Spin diameter adjustment on the SpinArc gun.

source and the preconfigured waveforms settings provided good spatter-free metal transfer across all of the tests. The tip-to-work distance was set at 19 mm (¾ in.), and the arc length did vary slightly depending on the shielding gas. As noted above, by using a constant arc trim value, the average power and heat input remained approximately constant at each WFS and TS constant deposit area test combination.

A SpinArc® MA-400 welding gun was used to complete all welding tests in this project. The spin diameter was adjusted on the welding gun by removing the base of the gun and rotating a knob to the desired spin diameter. The adjustment of the spin diameter can be observed in Fig. 2. The spin diameter was set to one and the spin frequency was set to zero for BOP tests without rotation; the conventional pulse was GMAW stringer beads. Spin frequency and the direction of spin were adjusted on the Bug-O tractor, which included a module that interfaced with the SpinArc welding gun. The tractor allowed for precise control of the TS and offered the ability to adjust both the welding gun and the work angle when groove welding.

ER5183 BOP Test Conditions

For all the tests, the majority of the welding parameters were held constant throughout the bead shape study. These parameters included gun angle, work angle, contact tip-to-work distance, and deposit area by using a contact WFS/TS ratio. For the shielding gas BOP study, the only variable adjusted on the power source was the WFS (Table 1). Both the gun angle and the work angle were held constant at 0 deg for the BOP tests. For the REP-GMAW BOP study, the ratio of spin frequency to TS (rotations/in.) was held constant to yield a similar underbead profile per unit length for comparison. Two spin diameters were selected to provide a noticeable effect on bead shape at each power level. A spin

diameter setting of 2 had improved fusion depth profiles and enhanced toe fusion compared to welds made with no arc rotation across all power levels. Welds made with a spin diameter setting of 4 resulted in slightly improved fusion depth profiles but had poorer weld reinforcement profiles due to the higher spin velocity and centrifugal force transferred to the weld pool. These two spin diameters were evaluated at the same three WFSs using pure argon. The spin frequency for the REP-GMAW BOP tests was adjusted to achieve a constant number of 50 rotations (spins) per in., which produced smooth weld surfaces. It should be noted that the REP gun was capable of generating spatter from excessive centrifugal force at very high spin frequency and diameter settings. BOP tests evaluated the effects of low, medium, and high power levels by changing the WFS from 225 to 300 to 375 in./min, respectively. Even though the goal was constant power tests via constant power source waveform and arc trim settings, the average power measured from the machine's meters varied slightly at each WFS level.

Table 1 — Shielding Gas Bead-on-Plate and Electrode Rotation Study Parameters

Trial	Wire Feed Speed (in./min)	Travel Speed (in./min)	A	V	Heat Input (kJ/in.)	Frequency (RPM)
Pure Argon						
Low power	225	11.25	162	21.1	18.23	n/a
Medium power	300	15	225	23.2	20.88	n/a
High power	375	18.75	282	25.2	22.74	n/a
75% Ar-25% He						
Low power	225	11.25	150	22	17.6	n/a
Medium power	300	15	211	23.9	20.17	n/a
High power	375	18.75	270	26.1	22.55	n/a
50% Ar-50% He						
Low power	225	11.25	149	22	17.48	n/a
Medium power	300	15	207	24.5	20.29	n/a
High power	375	18.75	262	26.7	22.39	n/a

BOP Metallographic Evaluation

BOP tests were extracted from the base plate using a band saw. Each BOP test sample was mounted in Bakelite™ before being polished to a 1-micron surface finish. Each sample was then etched to display the bead shape using Keller's reagent, which consists of distilled water, nitric acid, hydrochloric acid, and hydrofluoric acid. Samples were then imaged using both a light microscope and a stereoscope to observe both the bead shape and the fusion characteristics of the welds.

The BOP cross sections were used to measure bead fusion depth (BFD), bead width (BW), and bead height (BH); toe angle; weld toe incomplete fusion; and BMD — Fig. 3. BFD was measured from the top of the base material to the lowest point of fusion depth of the weld. The BW was measured at the point where the weld bead intersected with the top of the base material. BH was the maximum reinforcement above the base material plane. BMD was calculated as the area of fusion depth divided by the area of fusion depth plus the area of reinforcement. Incomplete fusion at the weld toe was the

Table 1 — (continued)

| Trial	Wire Feed Speed (in./min)	Travel Speed (in./min)	A	V	Heat Input (kJ/in.)	Frequency (RPM)
Pure Helium						
Low power	225	11.25	149	21.3	16.93	n/a
Medium power	300	15	199	24	19.1	n/a
High power	375	18.75	255	27.3	22.28	n/a
Spin Diameter 2						
Low power	225	11.25	156	21	17.47	550
Medium power	300	15	221	23.3	20.6	750
High power	375	18.75	290	24.7	22.92	950
Spin Diameter 4						
Low power	225	11.25	163	21.1	18.34	550
Medium power	300	15	232	22.6	20.97	750
High power	375	18.75	289	24.8	22.94	950
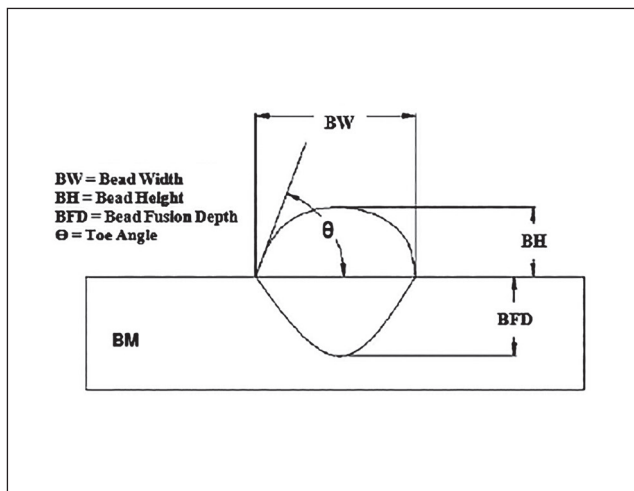
Fig. 3 — Schematic drawing of weld bead cross-section measurements.

average of the linear toe discontinuity along the base metal surface observed on both toes.

Results

The shielding gas BOP bead shape study evaluated GMAW-P stringer beads that were deposited using argon, argon-helium, and helium shielding conditions. For each GMAW-P shielding condition, the effects of weld power were evaluated by using three WFS and TS levels. In general, as power increased, the degree of melting increased in constant deposit area tests because the melting efficiency at constant heat input increased with increasing TS. Bead shape measurements were made to evaluate the effects of power and shielding conditions and compared to the REP-GMAW tests. The REP-GMAW BOP tests were deposited with pure argon shielding. Screening tests were used to determine the preferred spin diameter relative to the weld deposit width. Argon shielded BOP tests were then made with spin diameter settings of 2 and 4 and compared to the shielding gas condition BOP tests.

Shielding Gas BOP GMAW-P Study

Four shielding gases were used with no arc rotation to understand how shielding gas composition impacted the resulting fusion depth, BW, and fusion characteristics. The parameters and calculated heat input for each of the shielding gas study test conditions are provided in Table 1. The heat input was based on TS, average voltage, and amperage meter readings and was not calculated using a high-speed data acquisition system, which is needed to measure true power in waveform processes (Ref. 21). As the WFS was increased in 75 in./min increments for each shielding gas condition, the resulting heat input was increased by 2–3 kJ/in. The heat input ranged from 16.9 to 18.25 kJ/in. at low power (225 in./min WFS) to 19.1 to 20.9 kJ/in. at medium power (300 in./min WFS) to 22.3 to 22.7 kJ/in. at high power (375 in./min WFS) using the contact deposit area and arc trim setting approach.

Bead shape measurements (Table 2) were made on each weld cross section — Fig. 4. The BFD, BW, and BMD increased as the power (WFS) was increased for each shielding gas condition. As shown in Fig. 4, pure helium shielding had the greatest fusion depth, BW, and BMD at each power level. The BW showed the least sensitivity to shielding gas type at each power level. The BW ranged from 9.9 to 11.2 mm (0.38 to 0.44 in.) at low power to 13.5 to 14.4 mm (0.53 to 0.56 in.) at medium power to 15.2 to 16.6 mm (0.59 to 0.65 in.) at high power. The maximum BW difference was only 1.4 mm (0.05 in.) and recorded at the high-power level setting between helium and 50% argon-50% helium shielding conditions. The fusion depth ranged from 1.8 to 2.6 mm (0.07 to 0.1 in.) at low power to 3.0 to 4.2 mm (0.11 to 0.16 in.) at medium power to 4.2 to 7.1 mm (0.16 to 0.27 in.) at high power. The maximum fusion depth difference was 2.9 mm (0.11 in.) and recorded at the high power setting between helium and 50% argon-50% helium shielding conditions. The BMD ranged from 27.9 to 38.1% at low power to 41.6 to 52.3% at medium power to 51.2 to 67.2% at high power. The minimum BMD was expected with pure argon. The BMD dilution was expected to increase with helium additions where pure helium would provide the maximum BMD. The BMD did increase with increasing helium additions at low and medium power but had conflicting trends at high power.

The BMD depicts the percentage of base material diluted in the weld cross-section area and is an indicator of fusion quality. As power levels were increased across all shielding gas conditions, the BMD and fusion depth increased with these constant deposit area tests. Pure helium did provide the maximum BW, BFD, and BMD for all power (WFS) levels, but mixed results were seen between argon and the argon-helium mixtures.

While the welds made using pure helium shielding had the deepest BFD, there was still some finger fusion depth — Fig. 4. Finger fusion depth is characterized by a weld bead that's shaped like a mushroom, where there is deep center fusion depth and shallower fusion depth toward the weld toes. In addition to finger fusion depth, welds fabricated without arc rotation also had issues with weld toe incomplete fusion (Table 2). Weld toe incomplete fusion was examined and measured using optical microscopy; examples are shown in Fig. 7. Weld toe incomplete fusion was observed on all low power (WFS) test conditions for all shielding gas conditions. At low power levels, weld toe incomplete fusion varied from an average of 0.52 mm (0.02 in.) with pure argon to 0.23 mm (0.009 in.) with pure helium. Welds made using pure argon and 75% argon-25% helium had issues with incomplete fusion at the toes across all power levels. In this case, the weld toe incomplete fusion was greater than 0.35 mm (0.013 in.). Even with pure helium in the shielding gas mixture, the high-power condition was not able to mitigate weld toe incomplete fusion. Weld toe incomplete fusion is a planar defect and can reduce fatigue strength as well and may need to be mitigated for high-integrity applications. While the weld toe incomplete fusion defects were small and most would be difficult to identify with penetrant testing, they did assist in analyzing how the heat field spread throughout the arc.
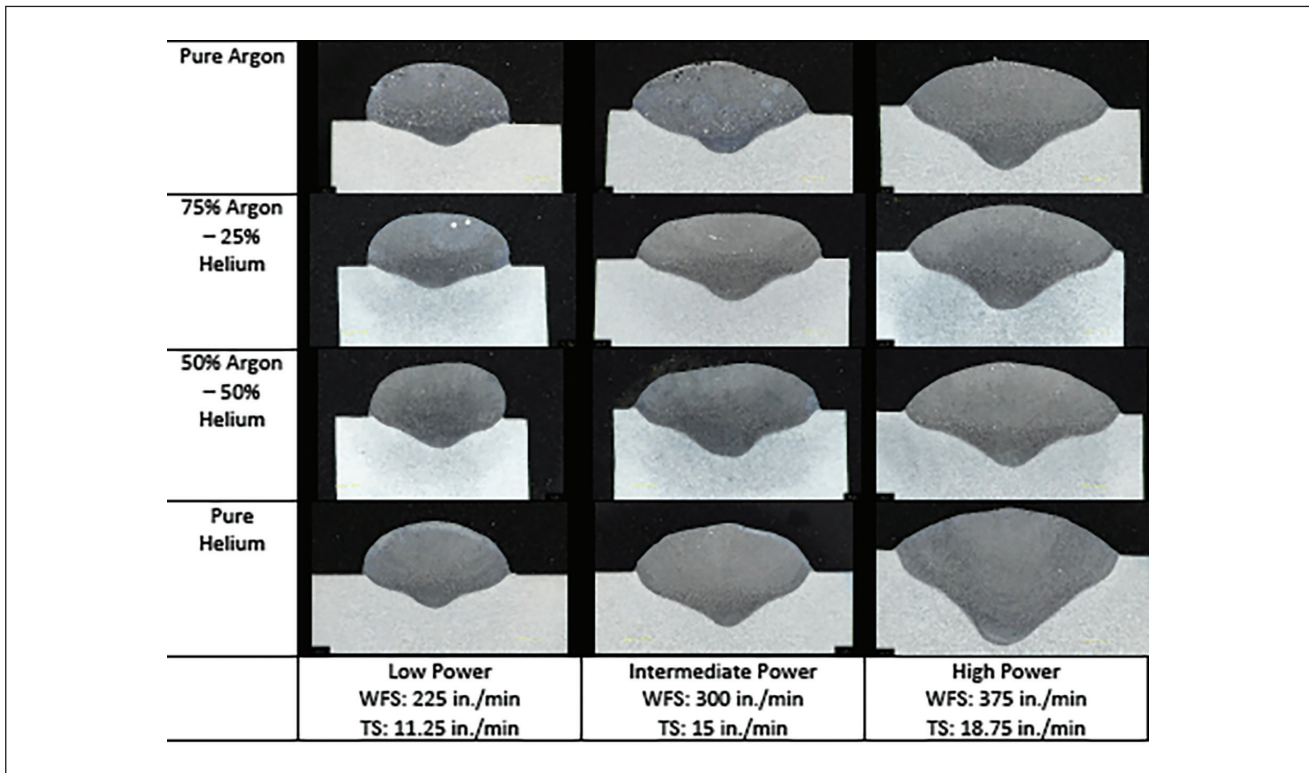
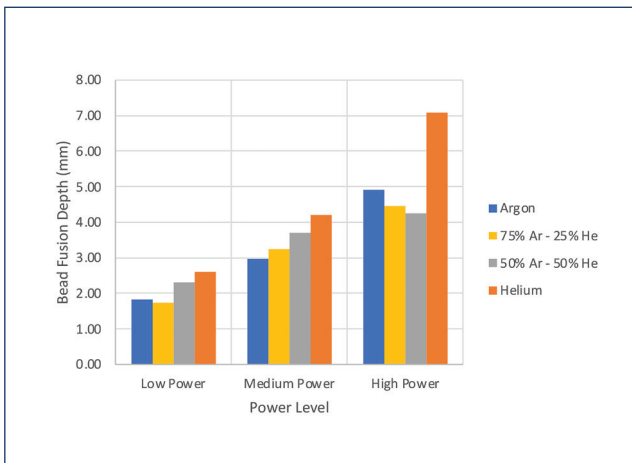*Fig. 4 — Weld cross-section bead shape map for the shielding gas BOP study.*

Fig. 5 — BFD at different power (WFS) levels for four shielding gases.
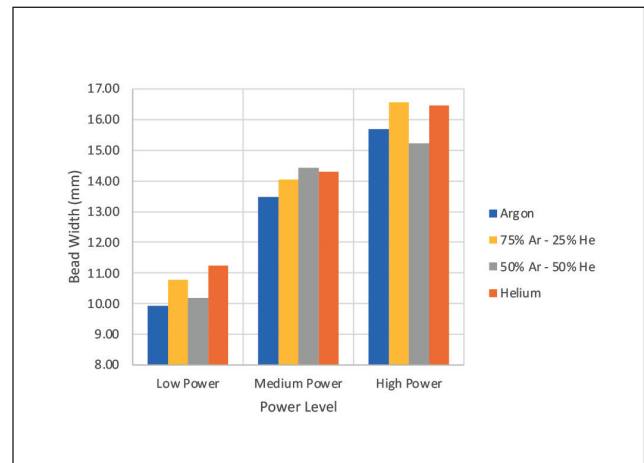

Fig. 6 — BW at different power (WFS) levels for four shielding gases.

REP-GMAW BOP Tests

The shielding gas BOP study results were then compared to the REP-GMAW BOP tests with different spin conditions and pure argon shielding gas (Table 3). The spin parameters had little effect on the calculated average power and heat input for each power (WFS) level. The heat input ranged from 17.5 to 18.3 KJ/in. at low power to 20.7 to 21 KJ/in. at medium power to 22.7 to 22.9 KJ/in. at high power. When the spin diameter was set to 2, the deposits had a uniform width, an elliptical underbead shape, a minimized finger fusion depth, and reduced weld toe incomplete fusion — Fig. 8. At spin

diameter 2, the BOP tests had a smooth bead shape and did not produce spatter during welding. At spin diameter 4, the BOP tests had smooth edges, but the weld reinforcement was biased as a result of higher centrifugal force due to the larger spin diameter at 50 rotations/in. spin frequency. The bias may be a benefit for out of position welding to offset the effects of gravity and will be discussed later.

The BFD, BW, and BMD were measured from the cross sections (Table 3). The fusion depth (mm) varied from 1.55 (spin diameter 4) to 1.8 (no spin) at low power to 3.0 (no spin) to 3.3 (spin diameter 4) at medium power to 4.9 to 5.1 at high power. The electrode rotation reduced the centerline fusion

Table 2 — Bead Fusion Depth, Width, and Base Metal Dilution for Gas Shielding Bead-on-Plate Study

Condition	Bead Fusion Depth (mm)	Bead Width (mm)	Base Metal Dilution (%)	Left Toe Incomplete Fusion (mm)	Right Toe Incomplete Fusion (mm)	Average Toe Incomplete Fusion (mm)
Pure Argon						
Low power	1.828	9.92	27.94	0.37	0.67	0.52
Medium power	2.967	13.49	41.61	0.39	0.81	0.60
High power	4.913	15.68	57.36	0.46	0.46	0.46
75% Ar-25% He						
Low power	1.739	10.79	29.85	0.31	0.54	0.42
Medium power	3.239	14.04	47.60	0.50	0.35	0.42
High power	4.446	16.55	55.13	0.31	0.39	0.35
50% Ar-50% He						
Low power	2.304	10.19	34.08	0.26	0.44	0.35
Medium power	3.696	14.44	51.06	0.15	0.30	0.23
High power	4.250	15.22	51.72	0.22	0.31	0.26
Pure Helium						
Low power	2.609	11.23	38.10	0.20	0.26	0.23
Medium power	4.216	14.30	52.28	0.31	0.17	0.24
High power	7.076	16.46	67.25	0.20	0.11	0.15

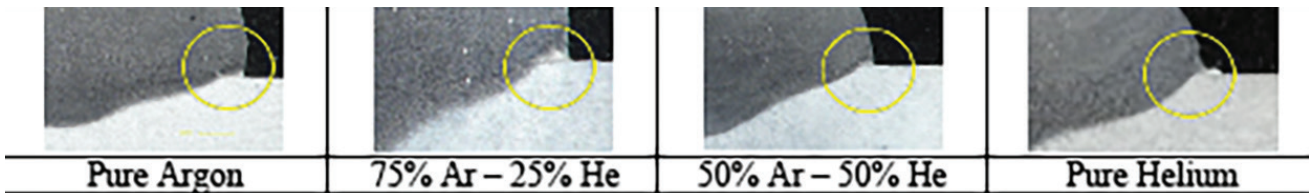Fig. 7 — *The weld toe incomplete fusion macrographs in the constant deposit area BOP shielding gas study at low power levels.*

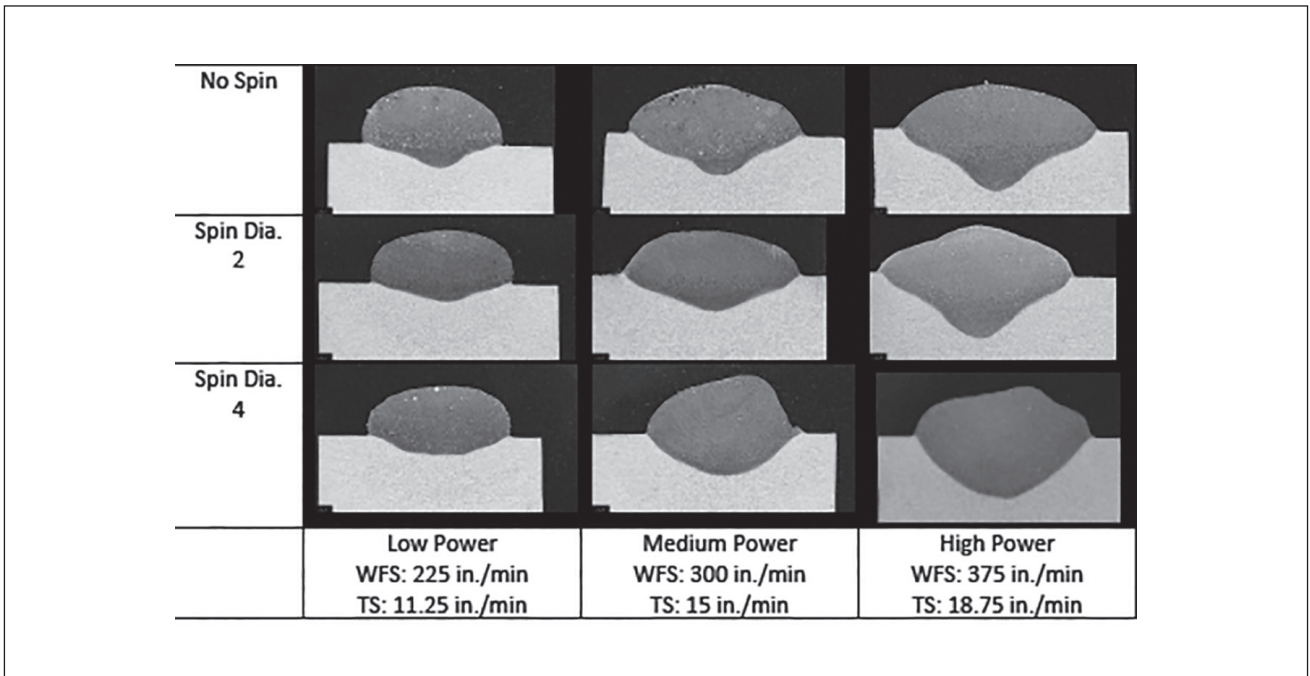| | Pure Argon | 75% Ar – 25% He | 50% Ar – 50% He | Pure Helium |

Fig. 8 — *Weld cross-section bead shape map for different spin conditions using argon shielding gas. Spin direction into page (left) and out of page (right) for each bead section.*

depth the most at low power and had less effect at medium and high power. The underbead shape for spin diameter 4 conditions had an elliptical profile, which is preferred for maximum fusion quality in multipass groove welds. However, weld reinforcement was biased toward the bead side where the spin direction was aligned with the travel direction. This reinforcement bias was due to the higher centrifugal force that is created with larger spin diameters at 50 spins/in. In hindsight, a lower spin frequency may reduce the reinforcement bias and is an area for future work at larger spin diameters and higher TSs.

The BW (mm) varied from 9.92 (no spin) to 9.82 (spin diameter 2) to 11.14 (spin diameter 4) at low power, from 13.49 (no spin) to 14.02 (spin diameter 2) to 12.51 (spin diameter 4) at medium power and from 15.58 (no spin) to 14.75 (spin diameter 2) to 13.63 (spin diameter 4) at high power. The BMD was fairly uniform across rotating electrode conditions at each power level using pure argon shielding. The BMD % varied from 25.85 (spin diameter 2) to 28.4 (spin diameter 4) at low power to 41.6 (no spin) to 44.5 (spin diameter 2) at medium power to 55.28 (spin diameter 4) to 57.4 (no spin). These small BMD changes at each power level showed no effect of spin.

Overall, the benefits of spin are an improvement in underbead shape at the weld toes and reduced toe incomplete fusion compared to welds fabricated with no arc rotation (Table 3). At both spin diameter settings, toe incomplete fusion was reduced even in low-power tests. Weld toe incomplete fusion (mm) varied from 0.52 to 0.29 at low power to 0.60 to 0.05 at medium power to 0.46 to 0.11 at high power — Fig. 11. Here, the REP-GMAW tests' weld toe incomplete fusion was significantly lower than that of the argon stringer BOP tests, and weld toe incomplete fusion was the same or smaller compared to welds made with pure helium shielding. Overall, the rotating electrode BOP tests had the best underbead shape.

As noted before, at large spin diameters and frequencies, reinforcement was biased on the side where the spin direction was aligned with TS direction. The bias was not desirable for flat position welds but was found to be a benefit when welding in the horizontal position. Preliminary weld tests found that smooth weld profiles could be produced on ceramic backing and in multipass deposition by aligning the spin direction with the top toe in the direction of travel. The spin centrifugal force is believed to offset the effects of gravity and will be discussed in the following section.

Table 3 — Weld Bead Fusion Depth, Width, and Base Metal Dilution Using Argon Shielding Gas Comparing GMAW-P with No Spin to REP-GMAW at Spin Diameter Settings of 2 and 4

| Condition	Bead Penetration (mm)	Bead Width (mm)	Base Metal Dilution (%)	Left Toe Incomplete Fusion (mm)	Right Toe Incomplete Fusion (mm)	Average Toe Incomplete Fusion (mm)
No Spin						
Low power	1.83	9.92	27.94	0.37	0.67	0.52
Medium power	2.97	13.49	41.61	0.39	0.81	0.60
High power	4.91	15.68	57.36	0.46	0.46	0.46
Spin Diameter of 2						
Low power	1.50	9.82	25.85	0.39	0.46	0.42
Intermediate power	2.90	14.02	44.50	0.15	0.13	0.14
High power	5.11	14.75	56.22	0.35	0.17	0.26
Spin Diameter of 4						
Low power	1.55	11.14	28.37	0.28	0.30	0.29
Intermediate power	3.34	12.51	41.94	0.09	0.00	0.05
High power	4.88	13.63	55.58	0.13	0.09	0.11
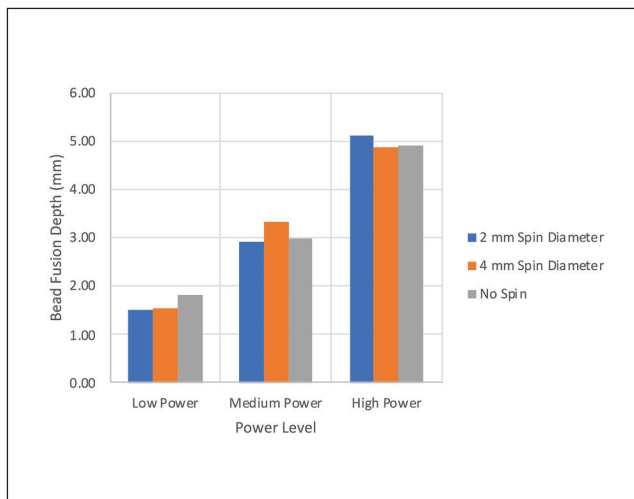
Fig. 9 — BFD at varying power levels (WFSs) for different spin diameters using pure argon shielding.
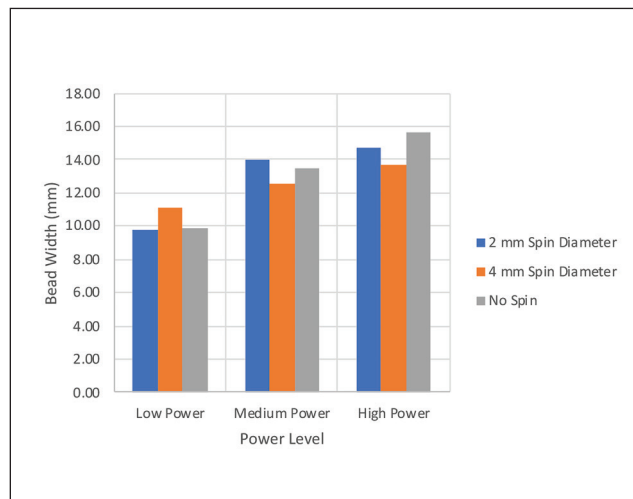

Fig. 10 — BW at varying power levels (WFSs) for different spin conditions using pure argon shielding.

Discussion

Benefits of REP-GMAW

Throughout the course of this project, multiple benefits of REP-GMAW technology were discovered. It was found that by employing the REP-GMAW process, welds could be fabricated with pure argon shielding gas that matched the fusion depth profile of traditional GMA welds fabricated with pure helium shielding gas. This allows for the realization of significant cost savings as helium is a finite resource and costs five times as much as pure argon shielding.

In addition to improving the fusion depth profile of the resultant weldment, the REP-GMAW process also assisted in improving weld quality. This quality improvement came in the form of reducing toe incomplete fusion. Weld toe incomplete fusion is a consistent issue when welding aluminum on thick plate and filling grooves with multiple welding deposits. Helium additions to the argon shielding gas promote a more efficient arc heat distribution, which allows for improved fusion and BMD along the weld toes. This study found that REP-GMAW welds fabricated with pure argon shielding resulted in fusion depth profiles similar to traditional GMAW-P welds fabricated with pure helium shielding. This allows for welds of the same quality and bead shape to be made with significant cost reductions resulting from the switch from helium to argon shielding gas.

Preferred Spin Conditions

The BOP bead shape measurements can be used to determine preferred REP-GMAW parameters. The BMD can be used to determine the preferred power (WFS) level to ensure adequate fusion depth and underbead profile and minimize the weld toe incomplete fusion. Overall, the medium and high power settings provided BMDs of 42–44% and 55–57%, respectively. These are preferred BMD levels to ensure complete fusion with the base material and minimize weld toe

incomplete fusion. Flat position applications can use high power whereas horizontal parameters require better parameter selection to achieve good fusion and bead reinforcement profile. Two spin diameter conditions were analyzed in this study, 2 and 4 mm (0.07 and 0.15 in.). A spin diameter of 2 was selected to develop preliminary butt joint procedures as it facilitated improvements in underbead shape and reduction of incomplete fusion at the weld toes. A spin diameter of 4 also produced similar benefits, but higher power and spin frequency combinations resulted in significant reinforcement bias. To ensure 50 spins/in., the spin frequency was increased from 550 to 950 RPM as travel was changed from 11.25 to 18.75 in./min, respectively. Lower spin frequencies, as low as 10–15 spins/in., are feasible and offer potential for tailoring bead shape for different application.

Future work should investigate the effects of rotating electrode conditions on bead shape for a range of deposit sizes needed for production groove and position applications. High-speed video should be used to develop relationships between the rotating arc on weld pool behavior, bead shape, and quality in different joint and position applications.

With pure argon, stringer bead aluminum GMA welds have a deep fusion depth profile at the center of the bead while there is minimal weld penetration at the weld toes. The arc rotation provided by the REP-GMAW process allows for a more concentric elliptical and favorable fusion depth profile. Overall, argon shielded REP-GMAW is a feasible alternative to helium shielded GMAW procedures for welding thick aluminum plate applications.

Conclusions

This work evaluated the potential for bead shape improvements and cost savings through the implementation of REP-GMAW of aluminum using pure argon shielding gas. The following conclusions can be drawn from this study:

1) Pure argon and 75% Ar-25% helium BOP deposits had toe incomplete fusion and narrower fusion depth profiles

compared to those of pure helium BOP deposits made with no electrode rotation.

    2) The REP-GMAW technology improved BOP bead shape and weld toe fusion compared to nonrotated stringer beads made with GMAW-P using pure argon shielding.

    3) The BFD profiles of pure argon REP-GMAW BOP welds that used preferred electrode rotation parameters were similar to those of pure helium nonrotated stringer beads.

    4) Electrode rotation promoted a nonsymmetric profile with deposit bias on the bead side where rotation direction was aligned with travel direction. This reinforcement bias increased with increasing spin diameter and frequency.

Acknowledgments

References

1. American Welding Society and American National Standards Institute. 2004. *Guide for Aluminum Hull Welding*. Miami, Fla.

2. Fortain, J. M., and Gadrey, S. 2013. How to select a suitable shielding gas to improve the performance of MIG and TIG welding of aluminium alloys. *Welding International* 27(12): 936–947. DOI: 10.1080/09507116.2012.753257

3. Essers, W. G., and Walter, R. 1981. Heat transfer and penetration mechanisms with GMA and plasma-GMA welding. *Welding Journal* 60(2): 37-s to 42-s.

4. Giedt, W. H., Tallerico, L. N., and Fuerschbach, P. W. 1989. GTA welding efficiency: Calorimetric and temperature field measurements. *Welding Journal* 68(1): 28-s to 30-s.

5. Eagar, T. W. 1990. The physics of arc welding processes. *Advanced Joining Technologies*. Dordrecht: 61–68. DOI: 10.1007/978-94-009-0433-0_5

6. Cai, C., He, S., Chen, H., and Zhang, W. 2019. The influences of Ar-He shielding gas mixture on welding characteristics of fiber laser-MIG hybrid welding of aluminum alloy. *Optics Laser Technology* 113(5): 37–45. DOI: 10.1016/j.optlastec.2018.12.011

7. American Welding Society. Weisman, C., ed. 1976. *Welding Handbook*, 7th Ed. Miami, Fla.: American Welding Society.

8. Mvola, B., and Kah, P. 2017. Effects of shielding gas control: Welded joint properties in GMAW process optimization. *International Journal of Advanced Manufacturing Technology* 88(9–12): 2369–2387. DOI: 10.1007/s00170-016-8936-2

9. Suban, M. Sep. 1998. Influence of hydrogen in argon as a shielding gas in arc welding of high-alloy stainless steel. Annual Assembly of the International Institute of Welding. Hamburg, Germany.

10. Dunn, G. J., and Eagar, T. W. Oct. 1986. Metal vapors in gas tungsten arcs: Part II. Theoretical calculations of transport properties. *Metallurgical and Materials Transactions A* 17(10): 1865–1871. DOI: 10.1007/BF02817282

11. Dunn, G. J., Allemand, C. D., and Eagar, T. W. Oct. 1986. Metal vapors in gas tungsten arcs: Part I. Spectroscopy and monochromatic photography. *Metallurgical and Materials Transactions A* 17(10): 1851–1863. DOI: 10.1007/BF02817281

12. Giedt, W. H., Tallerico, L. N., and Fuerschbach, P. W. 1989. GTA welding efficiency: Calorimetric and temperature field measurements. *Welding Journal* 68(1): 28-s to 30-s.

13. Eagar, T. W. 1990. The physics of arc welding processes. *Advanced Joining Technologies*. Dordrecht: 61–68. DOI: 10.1007/978-94-009-0433-0_5

14. Raju, D. L., and Raju, G. N. 2016. Effect of using a rotating electrode in gas metal arc welding on weld bead characteristics of Aluminium Alloy 6061-T6 weldments. *Proceedings of the World Congress on Engineering*, 4. Vol II WCE 2016. London, U.K.

15. Guo, N., Lin, S., Gao, C., Fan, C. L., and Yang, C. L. 2009. Study on elimination of interlayer defects in horizontal joints made by rotating arc narrow gap welding. *Science and Technology of Welding and Joining* 14(8): 584–588. DOI: 10.1179/136217109X456942

16. Vara Prasad, V., Madhu Babu, C., and Ajay, P. 2018. A review on rotating arc welding process. *Materials Today: Proceedings* 5(2): Part 1, pp. 3551–3555. DOI: 10.1016/j.matpr.2017.11.603

17. Dorasila, S., Rao, D. C. S., and Lingaraju, D. D. April 2016. An experimental investigation on design and development of rotational arc welding machine and parametric study on process variables. *International Journal of Scientific Engineering and Technology Research* 05(08): 5.

18. Kumar, S., Pedapati, S. R., and Ramakrishna, A. 2011. Effects of eccentricity and arc rotational speed on weld bead geometry in pulsed GMA welding of 5083 Aluminum Alloy. *Journal of Mechanical Engineering Research* 3: 186–196.

19. Kumar, R., Dilthey, U., Dwivedi, D. K., and Ghosh, P. K. 2009. Thin sheet welding of Al 6082 Alloy by AC pulse-GMA and AC wave-pulse-GMA welding. *Materials & Design* 30(2): 306–313.

20. Ovchinnikov, V. V., Drits, A. M., Kurbatova, I. A., and Rastopchin, R. N. 2016. Effect of controlled arc motion on the surface of a weld pool on the quality of a weld during argon-arc welding of a 1565chM aluminum alloy. *Russian Metallurgy* 2016(12): 1148–1154. DOI: 10.1134/S0036029516120144

21. The American Society of Mechanical Engineers. 2021. *BPVC Section IX — Welding, Brazing, and Fusing Qualification*. New York, N.Y.: ASME.

JIM HANSEN (*jhansen@ewi.org*) completed this work as part of a masters thesis in welding engineering at The Ohio State University and is currently employed in the arc welding and DED processes group at EWI, Columbus, Ohio. **DENNIS D. HARWIG** (*harwig.4@osu.edu*), PhD, is a research associate professor in the welding engineering laboratory at The Ohio State University and a senior technical leader for government programs as well as arc welding and DED processes at EWI, Columbus, Ohio.